Decoherence, delocalization, and irreversibility in quantum chaotic systems

K. Shiokawa[1,2] and B. L. Hu[1,2,3]
[1]*Department of Physics, University of Maryland, College Park, Maryland 20742*
[2]*Department of Physics, Hong Kong University of Science and Technology, Clear Water Bay, Kowloon, Hong Kong*
[3]*School of Natural Sciences, Institute for Advanced Study, Princeton, New Jersey 08540*
(Received 20 March 1995)

Decoherence in quantum systems which are classically chaotic is studied. The Arnold cat map and the quantum kicked rotor are chosen as examples of linear and nonlinear chaotic systems. The Feynman-Vernon influence functional formalism is used to study the effect of the environment on the system. It is well known that quantum coherence can obliterate chaotic behavior in the corresponding classical system. But interaction with an environment can under general circumstances quickly diminish quantum coherence and reenact classical chaotic behavior. How effectively decoherence works to sustain chaos, and how the resultant behavior qualitatively differs from the quantum picture, depend on the coupling of the system with the environment and the spectral density and temperature of the environment. We show how recurrence in the quantum cat map is lost and classical ergodicity is recovered due to the effect of the environment. Quantum coherence and diffusion suppression are instrumental to dynamical localization for the kicked rotor. We show how environment-induced effects can destroy this localization. Such effects can also be understood as resulting from external noises driving the system. Peculiar to decohering chaotic systems is the apparent transition from reversible to irreversible dynamics. We show such transitions in the quantum cat map and the quantum kicked rotor and distinguish them from apparent irreversibility originating from dynamical instability and imprecise measurements. By performing a time reversal on and following the quantum kicked rotor dynamics numerically, we show how the otherwise reversible quantum dynamics acquires an arrow of time upon the introduction of noise or interaction with an environment.

PACS number(s): 05.45.+b, 05.30.−d, 05.40.+j

I. INTRODUCTION AND SUMMARY

A. Quantum versus classical chaos

The problem of quantum chaos has been intensively studied in the recent decade [1–11]. Although the precise criteria for quantum chaos are still not well established at this stage, the salient features of a quantized classically chaotic system are better understood than before. In classical dynamics, chaos appears as the result of instability caused by nonlinearity or the compactness of the phase space, as manifested in the quantum kicked rotor and the Arnold cat map [6], two examples we will discuss in this paper. The degree of instability can be measured by the exponential rate of separation of initially infinitesimally close intervals, namely, the Lyapunov exponent. When this local instability occurs for the entire phase space, global chaos sets in. Ergodicity thus generated is one of the basic criteria for the validity of equilibrium statistical mechanics. (Infinite repetition of stretching and folding in the phase space may be the cause for the generation of self- organized structures in the microscopic world.)

In looking for similar phenomena in quantum systems one encounters basic difficulties. To begin with, the very concept of trajectories which is used to define classical chaos is meaningless in quantum mechanics. The equations of motion in quantum mechanics are linear. Seeking nonlinear effects in these linear equations as well as using concepts of determinancy in a theory based on probabilistic interpretations are intrinsically prohibitive. The words "quantum chaos" generally refer to possible traces or shadows of chaos in the quantum system obtained from quantizing the corresponding classical systems which are known to possess chaotic behavior. The study of quantum chaos is devoted to finding how the classical notion of instability changes when the system is quantized, and how such changes can be expressed in the language of quantum mechanics. For example, fingerprints of classical chaos may appear as scars in the wave function, as fluctuations in the spectrum, or as diffusion localization, etc. [6].

How are these classical and quantal characteristics related to each other in the correspondence between quantum and classical chaos? There are many criteria of classicality, an issue whose recent resurgence of interest is stimulated by developments in many areas of physics (see, e.g., [12]). Using the uncertainty principle as one criterion, we see immediately that there is a fundamental discrepancy between the definition of chaos and quantum uncertainty [13]. For systems with conservative dynamics, the initially infinitesimally separated trajectories in phase space will exponentially diverge in some direction and converge in some other direction. This will soon become incompatible with the quantum uncertainty principle which prevents one from specifying details between points in the phase space separated closer than the Planck constant h. Therefore the fact that many classi-

cally chaotic systems produce infinitely folded, Cantor-set structures which can continue to arbitrarily small scale due to nonlinearity is in conflict with quantum mechanics.

In classical mechanics, nonlinearity makes the dynamics sensitive to finer scales, leading to various fractal structures. However, in quantum mechanics, owing to the linear nature of Schrödinger's equation, one expects to see limitations to such fine structures. Quantum effects are known to smooth out the many-folded trajectories caused by nonlinearity. In this respect, the quantum effect is similar to the effect of noise on classically chaotic systems [14]. In fact, one can study the scaling property from the classical to the quantum regimes in a system when $\hbar \to 0$ as if the system is subject to some external noise [15].

B. Classicality as an emergent behavior of quantum open systems

The above description of quantum-classical correspondence takes the point of view that quantum effect is a correction to the underlying classical dynamics, which is the attitude taken by many works on this subject using semiclassical approximations. However, this is opposite to how nature works: most of us would agree that quantum mechanics is the fundamental theory which describes nature, and classical mechanics is only an approximation to it.

How classical dynamics arises from the fundamental principles of quantum mechanics and how our ordinary classical experience can be reconciled with the quantum depiction have been the basic questions asked in the foundation of quantum mechanics and in quantum measurement theory [16]. Although many different explanations exist, the environment-induced decoherence viewpoint seems to be one of simple and practical importance [17]. In this point of view, the quantum to classical transition is induced by the interaction of a quantum system with an environment. The averaged effect from coarse graining the large number of degrees of freedom is the diminution of quantum coherence and the appearance of diffusion and dissipation in the effective dynamics of the system. The decoherence time is defined as

$$t_{dec} = \frac{1}{\gamma}\left(\frac{\lambda_{\theta dB}}{\delta x}\right)^2 , \tag{1.1}$$

where γ is the damping constant, $t_{dis} = \gamma^{-1}$ is the dissipation time scale, $\lambda_{\theta dB} = h/\sqrt{2\pi mkT}$ is the thermal de Broglie wavelength, and δx is the characteristic size of the system (here we assume a coordinate coupling x). The decoherence time is usually very short for a bath at high temperatures. We refer the readers to recent reviews on this topic [17].

This approach has been applied to problems involving quantum decoherence in quantum measurement theory, mesoscopic physics, quantum cosmology, and semiclassical gravity [12]. However, the quantum and classical correspondence of chaotic systems in terms of environment-induced decoherence has so far been studied only by a limited number of authors [18–20].

C. Decoherence, localization, and irreversibility

1. *Noise and localization*

There are many detailed studies of the classical and quantum kicked rotor (QKR) model [6]. A particularly interesting feature of quantum nonlinear chaotic systems is the localization of wave functions in momentum space due to quantum coherence [23]. (The word "localization" here refers to Anderson localization [21], not to the establishment of δ-functional correlation between, say, the momentum and the coordinate in the realization of the quasiclassical state which is sometimes used in the context of decoherence and quantum to classical transition [22].) This momentum-space localization of the wave function is often compared with Anderson localization [21] of electrons in a random potential. Localization in the kicked rotor is considered to occur by a similar mechanism [24]. If one views classicality as an emergent behavior of a decohered quantum system, then it is of interest to study the effect of an environment on localization. Graham [25] studied the kicked rotor in a harmonic oscillator bath, and derived a master equation for the open system. His argument is mainly focused on the effect of dissipation induced by the environment. He used a low temperature approximation and in the zero temperature limit he claims that the dynamics becomes Markovian. This rather unusual behavior is due to the special non-Ohmic environment he used. In general, the Markovian regime corresponds only to an Ohmic bath at high temperature. Cohen and Fishman [26] used the influence functional method [27] to study the effect of noise associated with an Ohmic bath on localization for QKR and a similar model. They calculated explicitly the diffusion constant and the relevant time scales in terms of the noise correlation and the nonlinear parameter. On a related problem, Ott, Antonsen, and Hanson [28] first showed numerically that external noise breaks the localization of a wave packet in the QKR. Cohen also studied the effect of noise correlations [26]. Naively one does not expect correlations to play an essential role for chaotic systems because the memory in such systems is lost quickly. However, in the quantal case, long range correlations may alter the situation in a complicated way. In fact it is known that the appearance of noise autocorrelation depends on the system-environment coupling.

2. *Irreversibility*

Using a simple linear continuous model, the inverted harmonic oscillator potential, Zurek and Paz [19] recently observed that in the presence of noise, the dynamics can change from a reversible Liouville-type evolution to an irreversible one. We show that a similar behavior exists in the kicked rotor model. For a conserved Hamilto-

nian chaotic system, volume conservation causes a wave packet in phase space to contract exponentially in one direction. Without interaction with an environment, the other source of irreversibility intrinsic to chaotic systems arises from the limitation of actual measurements. For example, the classical kicked rotor behaves essentially irreversibly due to the instability of trajectories. However, in the quantal case, the system characterized by the quantum state becomes highly stable in spite of the nonlinearity of the Hamiltonian [32]. When this system interacts with an environment, there exists a sharp transition from a quantum reversible conservative stage to a classical irreversible stage. Irreversibility arising from finite precision associated with physical measurements will be replaced by irreversibility arising from coarse graining the environment.

D. Time scales of competing processes

One way to gauge the relative importance of the pertinent processes which can influence the dynamics of a quantum chaotic system is to compare their characteristic time scales. Let us start with cases with no interaction with an environment. There are essentially two different time scales involved. One is the Ehrenfest time t_E and the other is the relaxation time t_R. The Ehrenfest time t_E is defined as the time within which the Ehrenfest theorem holds.

$$t_E \sim \frac{1}{\lambda} \ln \frac{\delta p(0)}{\hbar}, \tag{1.2}$$

where $\delta p(0)$ is the relevant initial (angular) momentum scale. Violation of the Ehrenfest theorem in the quantal case arises from the nonlinear terms in the potential which can be seen in the evolution (Kramer-Moyal) equation of the Wigner function:

$$\frac{\partial W(X,p)}{\partial t} = -\frac{2}{\hbar} H \sin\left[\frac{\hbar}{2}\left(\frac{\overleftarrow{\partial}}{\partial p}\frac{\overrightarrow{\partial}}{\partial X} - \frac{\overleftarrow{\partial}}{\partial X}\frac{\overrightarrow{\partial}}{\partial p}\right)\right] W(X,p) \tag{1.3}$$

$$= \{H, W\} + \sum_{n=1}^{\infty} (-1)^n \left(\frac{2}{\hbar}\right)^{2n} \frac{1}{(2n+1)!} \times \frac{\partial^{2n+1} H}{\partial X^{2n+1}} \frac{\partial^{2n+1} W}{\partial p^{2n+1}}, \tag{1.4}$$

where $\{\,\}$ is the Poisson bracket.

The appearance of localization arises from the discrete spectrum of the Hamiltonian. Thus the time it takes for the wave packet to localize is determined by how long it takes for the system to recognize the discreteness of the spectrum. A simple argument is given in [23]: Since l represents the effective number of modes scattered in the period $[0, 2\pi]$, the typical spacing is given by $\Delta\omega \sim 2\pi/l$. Thus after $t_R \sim 1/\Delta\omega \sim l$, the system localizes. (See also discussion in Sec. III C.)

Upon interaction with a bath, a system effectively decoheres at the decoherence time scale t_{dec} (1.1). Another time scale t_C arising from the coarse graining appears which also contributes to the violation of the Ehrenfest theorem. As discussed in [19], it determines the transition regime from the reversible classical Liouville dynamics to the irreversible dynamics embodied in the Second Law of Thermodynamics.

From our study, this picture also holds for the kicked rotor. In this case, we see the transition from the initial constant-entropy regime to the entropy-increasing regime. Because of the compactness of the space, we see entropy does not increase forever but will eventually saturate. After t_C, the evolution is no longer unitary. (Note that even if the evolution of the Wigner function is the same as that of the classical Liouville distribution function before t_E, one should not regard the system as in a classical state. (As shown in the examples of [33], the Ehrenfest theorem is neither necessary nor sufficient to define classicality. There are systems which evolve strictly quantum mechanically but the expectation values of the canonical variables obey classical equations; and there are models which do not satisfy the theorem but their evolution is essentially classical.)

Dynamical localization is completed at the relaxation time t_R. At decoherence time t_{dec}, coherence is destroyed up to the localization length. If $t_{dec} \gg t_R$, suppression of momentum diffusion due to quantum effects always exists and we will never see the classical state.

It is known that the evolution of the kicked rotor is not time reversible, while its quantized version is time reversible. This type of quantum stability is also considered to be one of the characteristics of quantum chaos. In a quantum system, irreversibility arising from limited precision in a measurement now no longer causes serious loss of information. Instead, interaction with a bath introduces the irreversibility due to the coarse graining for the quantal case.

In this paper, we study the quantum dynamics of two simple models which possess classical chaotic behavior, the Arnold cat map and the kicked rotor. By introducing linear coupling with a harmonic oscillator bath assumed to be Ohmic and at high temperature, we show how the effective dynamics of a quantum open system reveals the well-known classical chaotic behavior. In Sec. II, we examine the quantum cat map (QCM) of a system coupled to a harmonic bath. The system is known to be chaotic when the corresponding matrix for the map is hyperbolic. We use the influential functional method to study the effect of the environment on this system. By measuring the linearized entropy we show that the decoherence mechanism works more efficiently than the regular case, namely, the rate of decoherence is faster in the chaotic system. Decoherence rate in chaotic systems was also studied by Tameshitit and Sipe [18]. Peculiar to the quantum case is the recurrence behavior of physical quantities, resulting from the finiteness of the phase space points in the quantum map due to the quantization (because the phase space is periodic in both the coordinate and momentum). We show that interaction with an environment erases the recurrence in the hyperbolic map but not in the elliptic map. Thus both cases behave close to the corresponding classical limit.

In Sec. III, we examine the quantum kicked rotor as a prototype of nonlinear chaotic systems. Without inter-

action with a bath, the wave function shows localization arising from quantum coherence effects. Loss of coherence due to interactions with an environment shown by the decay of the off-diagonal components of a reduced density matrix is responsible for the breaking of localization. The decay rate increases as the noise strength associated with the environment and the nonlinear parameter get larger. In Sec. IV, we examine the transition from reversible to irreversible dynamics intrinsic to an unstable system due to its interaction with an environment. We show that the same mechanism holds for both the cat map and kicked rotor. For both cases, the entropy shows saturation possibly due to the bounded nature of the phase space. Furthermore, we perform time reversal numerically and show how the interaction with an environment changes the nature of irreversibility. Details of results can be found at the end of each section.

II. DECOHERENCE IN A LINEAR MAP

A. Quantum cat map

The cat map is a linear area-preserving map T on a two-torus in phase space formed identifying the boundaries of the interval $[0, 2\pi]$ in both the coordinate Q and the momentum P directions [34]. From time step j to $j+1$, it is given by

$$\begin{pmatrix} Q_{j+1} \\ P_{j+1} \end{pmatrix} = \begin{pmatrix} a & b \\ c & d \end{pmatrix} \begin{pmatrix} Q_j \\ P_j \end{pmatrix} = T \begin{pmatrix} Q_j \\ P_j \end{pmatrix} , \quad (2.1)$$

where $\det T = 1$ guarantees area preservation. The degree of chaos depends on the choice of T. The eigenvalues of T are either both real or both imaginary. In the latter case, T is elliptic, the motion becomes periodic, and no sensitive dependence on the initial condition is observed. When T is hyperbolic, the motion becomes chaotic.

The quantized cat map is studied in detail by Hannay and Berry [35]. Due to the periodicity and thus the discreteness of both phase space variables, the area of the torus is characterized by a discrete Planck's constant,

$$\hbar = 2\pi/\mathcal{N} , \quad (2.2)$$

where $\mathcal{N}$ is the number of sites in both the coordinate and the momentum directions in phase space. Because of this, quantum dynamics defined by the cat map is considered to describe quantum resonance. This is, however, not a generic feature for other systems which have continuous phase space.

The action $S(Q_{j+1}, Q_j)$ for this linear map is easily constructed from conditions

$$\frac{\partial S(Q_{j+1}, Q_j)}{\partial Q_{j+1}} = P_{j+1}, \quad -\frac{\partial S(Q_{j+1}, Q_j)}{\partial Q_j} = P_j . \quad (2.3)$$

Combining (2.1) and (2.3) gives

$$S(Q_{j+1}, Q_j) = \frac{1}{2b}(aQ_j^2 - 2Q_jQ_{j+1} + dQ_{j+1}^2) . \quad (2.4)$$

Before imposing the periodic boundary conditions, the propagator is

$$U(Q_{j+1}, Q_j) = \frac{1}{2\pi}\left(\frac{i\mathcal{N}}{b}\right)^{\frac{1}{2}} \exp\frac{i\mathcal{N}}{4\pi b}(aQ_j^2 - 2Q_jQ_{j+1} + dQ_{j+1}^2) . \quad (2.5)$$

With periodic boundary conditions, one needs to sum over all equivalent initial points, yielding

$$\begin{aligned} U(Q_{j+1}, Q_j) &= \frac{1}{2\pi}\left(\frac{i\mathcal{N}}{b}\right)^{\frac{1}{2}} \sum_{m=-\infty}^{\infty} \exp\left[\frac{i\mathcal{N}}{4\pi b}[a(Q_j + 2\pi m)^2 - 2(Q_j + 2\pi m)Q_{j+1} + dQ_{j+1}^2]\right] \\ &= C(T, \mathcal{N}) \exp\left[\frac{i\mathcal{N}}{4\pi b}[aQ_j^2 - 2Q_jQ_{j+1} + dQ_{j+1}^2]\right] , \end{aligned} \quad (2.6)$$

where $C(T, \mathcal{N})$ is a constant depending on the form of T and $\mathcal{N}$.

In fact, $C(T, \mathcal{N})$ vanishes in many choices of T and this sum gives a nontrivial value for the propagator only if the matrix has a special form. We choose

$$T_1 = \begin{pmatrix} 0 & 1 \\ -1 & 0 \end{pmatrix} \quad (2.7)$$

for the elliptic case, and

$$T_2 = \begin{pmatrix} 2 & 1 \\ 3 & 2 \end{pmatrix} \quad (2.8)$$

for the hyperbolic case.

For these special choices of the matrix elements T_1 and T_2, the propagators take on the simple form

$$U_1(j+1, j) = \sqrt{\frac{i}{\mathcal{N}}} \exp\left[-\frac{i}{\hbar}Q_jQ_{j+1}\right] , \quad (2.9)$$

$$U_2(j+1, j) = \sqrt{\frac{i}{\mathcal{N}}} \exp\left[\frac{i}{\hbar}(Q_j^2 - Q_jQ_{j+1} + Q_{j+1}^2)\right] . \quad (2.10)$$

Since each iteration describes a permutation among sites, each site belongs to a periodic orbit. Thus quantum evolution follows the classical dynamics, resulting in a recurrence of the wave function (or equivalently, of the Wigner function) [35].

B. Decoherence in the quantum cat map

We now couple the system to a bath of N harmonic oscillators linearly. (Nonlinearity in the coupling could enhance the interaction between the systems and the bath, as one mode in the system is coupled to many different modes in the bath. One thus expects that this increased degrees of freedom would help to decohere the system more efficiently than in the linear coupling case. Nonlinearity in the bath seems to have a similar effect [36].) The Hamiltonian of the bath of oscillators with coordinates q_α and momentum $p_\alpha (\alpha = 1, ..., N)$ is

$$H_B = \sum_{\alpha=1}^{N} \left(\frac{p_\alpha^2}{2} + \frac{\omega_\alpha^2 q_\alpha^2}{2} \right). \tag{2.11}$$

The interaction Hamiltonian between the system Q and the bath variables q_α is assumed to be bilinear,

$$H_C = \sum_{\alpha=1}^{N} C_\alpha Q q_\alpha, \tag{2.12}$$

where C_α is the coupling constant of the αth oscillator.

Integrating out the bath variables, we get the reduced density matrix,

$$\rho_r(Q_j, Q'_j, t) = \int \prod_{\alpha=1}^{N} dq_\alpha dq'_\alpha \exp \frac{i}{\hbar} [S(Q) + S_C(Q, q_\alpha) + S_B(q_\alpha) - S(Q') - S_C(Q', q'_\alpha) - S_B(q'_\alpha)], \tag{2.13}$$

where S is the classical action of the system defined in (2.4) and S_B and S_C are the actions for the bath and the coupling, respectively. The evolutionary operator J_r for the reduced density matrix from time step j to $j+1$ is

$$J_r(Q_{j+1}, Q'_{j+1} \mid Q_j, Q'_j, t) = \int DQDQ' \exp \frac{i}{\hbar} [S(Q) - S(Q') + A(Q, Q')] \tag{2.14}$$

in a path-integral representation [27,37–39], where

$$\frac{i}{\hbar} A(Q, Q') = \frac{1}{\hbar^2} \int_0^t ds \int_0^s ds' r(s) [-i\mu(s - s') R(s') - \nu(s - s') r(s')] \tag{2.15}$$

is the influence action. Here $r \equiv \frac{1}{2}(Q - Q')$, $R \equiv \frac{1}{2}(Q + Q')$, and $\mu(s), \nu(s)$ are the dissipation and noise kernels, respectively [39].

If we consider the simplest case of an Ohmic bath at high temperature $kT > \hbar\Lambda \gg \hbar\omega_\alpha$, where Λ is the cutoff frequency for the bath [37], and consider times shorter than the dissipation time, then we obtain a Gaussian form for the influence functional, with $\frac{i}{\hbar} A(Q, Q') = -\frac{2M\gamma kT}{\hbar^2} \sum_j r_j^2$ where the noise kernel becomes local, $\nu(s) = 2M\gamma kT\delta(s)$, γ is the damping coefficient. Because the chaotic trajectory washes out information about the past rapidly, we expect that memory effect would be less important in classically chaotic systems than classically regular systems. Nevertheless, in the quantal case in which the classical stretching and folding behavior is suppressed, it would still be interesting to study how the non-Markovian behavior competes with nonlinearity [26]. We will discuss this issue in the next section. The unit-time propagator becomes

$$J_r(Q_{j+1}, Q'_{j+1} \mid Q_j, Q'_j) = \langle J_r(Q_{j+1}, Q'_{j+1} \mid Q_j, Q'_j, \xi) \rangle = \left\langle \exp \frac{i}{\hbar} [S(Q_{j+1}, Q_j) - S(Q'_{j+1}, Q'_j) + 2\xi r_{j+1}] \right\rangle. \tag{2.16}$$

Here ξ is a Gaussian white noise given by

$$\langle \xi \rangle = 0, \quad \left\langle \exp \frac{2i}{\hbar} \xi r \right\rangle = \exp \left[-\frac{2M\gamma kT}{\hbar^2} r^2 \right], \tag{2.17}$$

where $\langle\ \rangle$ denotes a statistical average over noise realization ξ.

For the elliptic map, we get

$$J_r(Q_{j+1}, Q'_{j+1} \mid Q_j, Q'_j, \xi) = \left(\frac{i}{\mathcal{N}} \right)^{1/2} \exp \left[\frac{2i}{\hbar} (-r_j R_{j+1} - r_{j+1} R_j + \xi r_{j+1}) \right], \tag{2.18}$$

and for the hyperbolic map,

$$J_r(Q_{j+1}, Q'_{j+1} \mid Q_j, Q'_j, \xi) = \left(\frac{i}{\mathcal{N}} \right)^{1/2} \exp \left[\frac{2i}{\hbar} (2r_j R_j + 2r_{j+1} R_{j+1} - r_j R_{j+1} - r_{j+1} R_j + \xi r_{j+1}) \right]. \tag{2.19}$$

The Wigner function is defined as

$$W(R, p) = \frac{1}{\pi\hbar} \int_{-\infty}^{\infty} \psi(R + r) \psi^*(R - r) \exp[\tfrac{-2ipr}{\hbar}] dr, \tag{2.20}$$

where p is the momentum conjugate to r. The propagator K_T for the Wigner function is

$$K_T(R_{j+1}, p_{j+1} \mid R_j, p_j, \xi) = \frac{1}{\pi\hbar} \sum_{r_j} \sum_{r_{j+1}} J_r(Q_{j+1}, Q'_{j+1} \mid Q_j, Q'_j, \xi) \times \exp \frac{2i}{\hbar} (p_j r_j - p_{j+1} r_{j+1}). \tag{2.21}$$

This is reduced to the form of the classical cat map. For the elliptic case,

$$R_j = -p_{j+1} + \xi, \quad p_j = R_{j+1}. \tag{2.22}$$

For the hyperbolic case,

$$R_j = 2R_{j+1} - p_{j+1} + \xi, \quad p_j = -3R_{j+1} + 2p_{j+1} - 2\xi. \tag{2.23}$$

Thus, without the environment, quantum evolution follows classical permutation [35]. We can also say that the transformation from the classical map to the corresponding quantum propagator $T \to K_T(R_{j+1}, p_{j+1}|R_j, p_j, \xi = 0)$ preserves the group structure. When coupled to the bath, the cat map is exposed to a Gaussian noise from the environment in each time step. The phase space is divided by a finite number of different periodic orbits and the period is known to increase roughly proportional to $\mathcal{N}$. The discretized noise induces transition between different periodic orbits in an irregular way. As a consequence, the recurrence of the physical quantity will disappear in the quantum map and the classical type of mixing is regained.

Figure 1 shows $\mathrm{Tr}\rho_r^2$, the linearized entropy (with the reversed sign) for various cases. If there is no interaction with the environment, the entropy is constant for both the regular and chaotic cases. When interaction sets in, $\mathrm{Tr}\rho_r^2$ decays exponentially, showing that the system rapidly decoheres. There is no recurrence of this quantity observed. In spite of the discreteness of the points on the torus, we expect that the system behaves classically due to the influence of the environment.

Note that a regular system also decoheres in a similar manner, albeit with a slower rate [18]. These results indicate that if the underlying classical system shows chaotic behavior, even after quantization, the system still possesses the mixing behavior. This mixing property enhances the random perturbations from the environment, thus accelerating the suppression of quantum interference. However, in this particular example, the dynamics is essentially classical as is seen in (2.22,23) (in this case, the value of $\hbar$ comes in through the number of sites $\mathcal{N}$). More general cases should be examined.

In Fig. 2, we show the mean displacement of points in the phase space from the initial configuration as a function of time. This is defined by $l = \sqrt{\langle \Delta x^2 + \Delta p^2 \rangle}$, where Δx and Δp are the displacement from the initial phase space points, $\langle\,\rangle$ is the average over the phase space points and noise realizations. In the chaotic case, we see

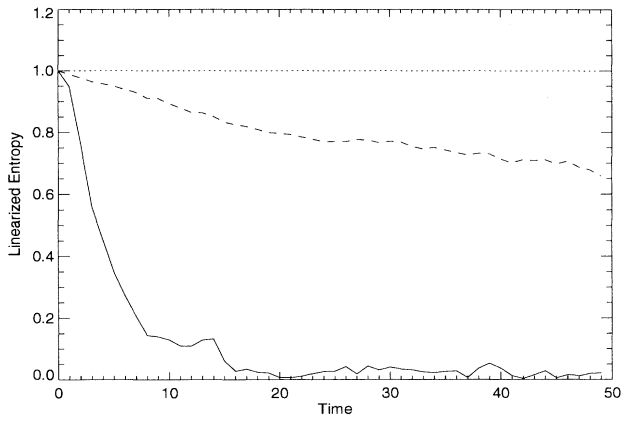

FIG. 1. The linearized entropy (with opposite sign) is plotted against time. If there is no environment, the entropy is constant for both the hyperbolic and elliptic cases, indicating the purity of the state (dotted line). For the hyperbolic map, even though classically this system is strongly chaotic, the corresponding quantum system does not show chaotic behavior. This situation changes drastically when the system interacts with a thermal bath. In this case, the entropy due to coarse graining keeps increasing. Note that in the hyperbolic case (solid line), the rate of entropy increase is larger than in the elliptic case (dashed line). $\mathcal{N} = 50$ is used here (also in Fig. 2).

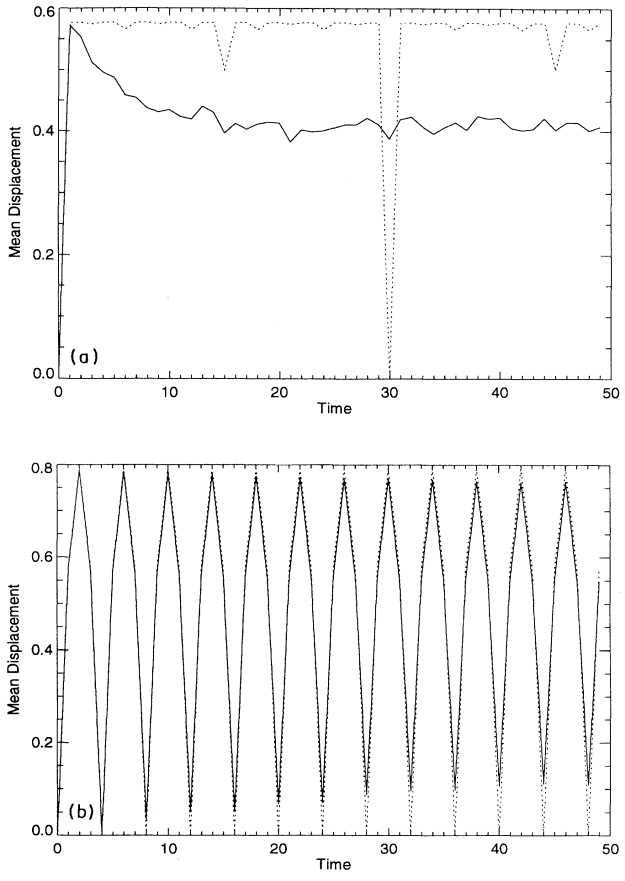

FIG. 2. The mean phase space point displacement is shown. When there is no environment (dotted line), the system shows recurrence in both the hyperbolic (a) and elliptic (b) cases. In the presence of an environment (solid line), the hyperbolic map loses the recurrence behavior under the Gaussian noise with $\sigma = 0.08$ and maintains a near-constant value, indicating ergodicity of the classical hyperbolic map. On the other hand, the elliptic map still shows recurrence with the same amount of noise, corresponding to the classical periodicity.

the recurrence disappears with just a small amount of noise [Fig. 2(a)], whereas in the regular case, the same amount of noise does not alter the qualitative picture of recurrence [Fig. 2(b)]. In both cases, the decohered quantum system behaves similarly to the classical picture in which the regular and chaotic dynamics are clearly distinguished. For the elliptic map, the classical dynamics is completely periodic. For the choice of T_1 in (2.7), the period is 4. On the other hand, for the hyperbolic map T_2 in (2.8), the classical dynamics is nonperiodic. In spite of the discreteness of the points on the torus, the system behaves effectively classically due to the effect of the environment.

III. NONLINEARITY AND DECOHERENCE

A. Quantum kicked rotor

The kicked rotor and its map version, known as the standard map, are one of the most intensively studied models from both the quantum and classical points of view [6]. The Hamiltonian of the kicked rotor is given by

$$H = \frac{p^2}{2m} + K\cos x \sum_{j=-\infty}^{\infty} \delta(t-j) \ , \tag{3.1}$$

which describes a one-dimensional rotor subjected to a δ-functional periodic kick at $t = j$. Here x is the angle of the rotor with period 2π, m is the moment of inertia, p is the angular momentum, and K is the strength of the kick and, in this case, the nonlinear parameter. When $K > K_c = 0.9716$, the system becomes chaotic over the entire phase space. The average energy $\langle p^2/2\rangle$ is known to show diffusive behavior like that of a Brownian particle under a stochastic force. This suggests the emergence of randomness in a deterministic chaotic system.

The quantum dynamics of the kicked rotor is depicted by the corresponding Schrödinger equation

$$i\hbar\frac{\partial}{\partial t}\psi(x,t) = -\frac{\hbar^2}{2m}\frac{\partial^2}{\partial x^2}\psi(x,t) + K\cos x \sum_{j=-\infty}^{\infty} \delta(t-j)\psi(x,t) \ , \tag{3.2}$$

where ψ is the wave function for the rotor. Denoting ψ_j as the wave function $\psi(x,t)$ at each discrete time $t = j$, and integrating (3.2) from j to $j+1$, we obtain

$$\psi_{j+1}(x) = \exp\left[-i\frac{\hbar}{2m}\frac{\partial^2}{\partial x^2}\right]\exp\left[-i\frac{K\cos x}{\hbar}\right]\psi_j(x) \ . \tag{3.3}$$

The quantum kicked rotor is known to exhibit dynamical localization. After some relaxation time scale, the wave function becomes exponentially localized in the momentum space [23]. This may be interpreted as a particle moving in a lattice with a quasirandom potential. This heuristic picture seems to justify the analogy between the quantum kicked rotor to the tight binding model with an exponentially decaying hopping parameter which is known to show Anderson localization. The explicit transformation to the tight binding model was constructed in [24]. In spite of the nonrandom, deterministic nature of the kicked rotor Hamiltonian, numerical results there assuming sufficient quasirandomness seem to support this analogy. Dynamical localization in this context arises from the suppression of classical diffusive behavior in the quantum dynamics. As shown by Ott *et al.* [28], a small external noise can break the localization. Numerically they observed three different regimes in the behavior of the diffusion constant D depending on the magnitude of noise. When the noise becomes sufficiently large, the system recovers the classical diffusive behavior.

It is of interest to interpret the above results due to noise from the microscopic open system point of view. When the system interacts with an environment, we know that coarse graining of the environmental variables is also a source of noise and dissipation. We shall now derive the influence functional for the quantum kicked rotor and study its behavior.

B. Quantum kicked rotor in a bath

Cohen and Fishman studied the case for the Ohmic bath in detail [26]. They calculated explicitly the diffusion constant and the relevant time scales in terms of the noise correlation and the nonlinear parameter.

We introduce a linear coupling of the system momentum p with each oscillator coordinate $q_\alpha (\alpha = 1, ..., N)$ in the bath in the form $H_C = \sum_{\alpha=1}^{N} C_\alpha q_\alpha p$ (here q, p without the subscript α denote the system coordinate and momentum variables). For an Ohmic environment, the action functional has the same form as (2.15), except that the coordinate variable Q there is now replaced by a momentum variable p.

$$\frac{i}{\hbar}A(p,p') = \frac{1}{\hbar^2}\int_0^t ds \int_0^s ds' p^-(s)[-i\mu(s-s')p^+(s') - \nu(s-s')p^-(s')], \tag{3.4}$$

where $p^\pm(s) = p(s) \pm p'(s)$.

In a similar way, we introduce the noise $\xi(\tau)$ such that

$$\left\langle \exp\left[-i\int \xi(\tau)p(\tau)\right]\right\rangle = \exp\left[-\frac{1}{\hbar}\int_0^t ds \int_0^s ds' p^-(s)\nu(s-s')p^-(s')\right] \ . \tag{3.5}$$

As before, we will examine processes in the time span where dissipation is small, thus ignoring the effect of the dissipation kernel $\mu(s)$.

Under these assumptions, the action of the noise kernel can be formally absorbed in the propagator for the wave function. The unit-time propagator for the wave function $U_\xi(j+1, j)$ is given by

$$U_\xi(j+1, j) = \exp\left[-\frac{iK\cos x}{\hbar}\right]\exp\left[-\frac{ip^2}{2m}\right] \times \exp\left[-\frac{i\xi p}{\hbar}\right] \ , \tag{3.6}$$

where, as before, the noise term ξ arises from using a Gaussian identity in the integral transform of the term involving the noise kernel in the influence functional [27]. Summing over all noise realizations $\langle\,\rangle$ gives the desired reduced density matrix

$$\rho_j(p,\ p') = \langle \psi_{j,\xi}(p)\ \psi^*_{j,\xi}(p') \rangle\ , \tag{3.7}$$

where

$$\psi_{j+1,\xi}(p) = U_\xi(j+1,\ j)\ \psi_{j,\xi}(p) \tag{3.8}$$

and $\psi_{j,\xi}(p)$ is the wave function under the influence of a particular noise history represented by ξ.

In the same way, $\mathrm{Tr}\rho_r^2$ can be expressed as

$$\mathrm{Tr}\rho_r^2 = \left\langle \sum_p \sum_{p'} \psi_\xi(p)\ \psi^*_\xi(p')\ \psi_{\xi'}(p')\ \psi^*_{\xi'}(p) \right\rangle_{\xi,\xi'}\ , \tag{3.9}$$

where $\langle\,\rangle_{\xi,\xi'}$ denote the statistical average of all possible noise histories of two independent noises $\xi(\tau), \xi'(\tau)$ defined at each interval from j to $j+1$. At high temperatures, $\xi(\tau), \xi'(\tau)$ are reduced to two time-uncorrelated independent Gaussian white noises defined at each time step.

There are many possible ways of introducing an interaction between the system and the bath, though many of them are related to each other as shown in [26]. One interesting case is to introduce a coupling through the coordinate x. Then to preserve periodicity of the Hamiltonian under the coordinate transformation $x \to x + 2\pi$, we need to restrict the range of noise to $\xi = n\hbar (n = 0, \pm 1, \pm 2, ...)$, or choose the interaction Hamiltonian to be $H_C = C_\alpha q_\alpha \cos(x)$. In the latter case, we may further assume the form $H_C = C_\alpha q_\alpha \cos(x + \phi_\alpha)$, where ϕ_α is the random phase [28], to remove the coordinate dependence of the interaction. However, they all give the same result, but with different noise correlations. For example, from (3.6) we can calculate the propagator $U_\xi(j,\ 1)$ from $t = 1$ to $t = j$ as

$$\begin{aligned} U_\xi(j,\ 1) &= U_\xi(j,\ j-1)\ U_\xi(j-1,\ j-2) \cdots U_\xi(2,\ 1) \\ &= \exp\left[-\frac{iK\cos x}{\hbar}\right] \exp\left[-\frac{ip^2}{2m}\right] \exp\left[-\frac{i\xi(j)p}{\hbar}\right] \exp\left[-\frac{iK\cos x}{\hbar}\right] \exp\left[-\frac{ip^2}{2m}\right] \exp\left[-\frac{i\xi(1)p}{\hbar}\right] \\ &= \exp\left[-\frac{i\eta(j)p}{\hbar}\right] \exp\left[-\frac{iK\cos[x+\eta(j)]}{\hbar}\right] \exp\left[-\frac{ip^2}{2m}\right] \cdots \exp\left[-\frac{iK\cos[x+\eta(1)]}{\hbar}\right] \exp\left[-\frac{ip^2}{2m}\right]\ , \end{aligned} \tag{3.10}$$

where $\eta(j) = \xi(j) + \cdots + \xi(1)$. Thus this describes the same dynamics as couplings through x via $H_C = C_\alpha q_\alpha \sin x$, as long as the noise $\eta(j)$ remains small. The correlations of the two different noises $\eta(j)$ and $\xi(j)$ are related by

$$\langle \eta(\tau)\eta(\tau') \rangle = \sum_{t=1}^{\tau} \sum_{t'=1}^{\tau'} \langle \xi(t)\xi(t') \rangle\ . \tag{3.11}$$

Note that even if ξ is a white noise, η is not necessarily white.

C. Localization and decoherence in the quantum kicked rotor

The eigenvalue equation for the quasienergy state in the QKR is given by [24]

$$\exp\left(-\frac{i}{\hbar}K\cos x\right) \exp\left(-\frac{i}{\hbar}\frac{p^2}{2m}\right) u_\omega(x) = \exp\left(-\frac{i}{\hbar}\omega\right) u_\omega(x). \tag{3.12}$$

This can be transformed to

$$\left\{\exp\left[-\frac{i}{\hbar}\left(\frac{p^2}{2m} - \omega\right)\right] \left[1 - i\tan\left(\frac{K\cos x}{2\hbar}\right)\right] - \left[1 + i\tan\left(\frac{K\cos x}{2\hbar}\right)\right]\right\} \left[1 + \exp\left(-\frac{i}{\hbar}K\cos x\right)\right] \frac{1}{2} u_\omega(x) = 0. \tag{3.13}$$

If we define $\bar{u}_\omega(x)$ as

$$\bar{u}_\omega(x) = \left[1 + \exp\left(-\frac{i}{\hbar}K\cos x\right)\right] \frac{1}{2} u_\omega(x) \tag{3.14}$$

then (3.13) can be written as

$$\left\{ i \frac{\{1 - \exp[-\frac{i}{\hbar}(\frac{p^2}{2m} - \omega)]\}}{\{1 + \exp[-\frac{i}{\hbar}(\frac{p^2}{2m} - \omega)]\} - \tan(\frac{K\cos x}{2\hbar})} \right\} \bar{u}_\omega(x) = 0. \tag{3.15}$$

Expanding $\bar{u}_\omega(x)$ as $\bar{u}_\omega(x) = \sum_{k=-\infty}^{k=\infty} \bar{u}_k e^{ikx}$, we get

$$T_k \bar{u}_k + \sum_{r\neq 0} W_r \bar{u}_{k+r} = E\bar{u}_k \ , \tag{3.16}$$

where

$$T_k = \tan\left(\frac{\omega}{2\hbar} - \frac{\hbar^{n-1}k^n}{4}\right) \ , \tag{3.17}$$

$$W_k = \frac{1}{2\pi}\int_0^{2\pi} d\theta e^{ik\theta} \tan\left(\frac{K\cos x}{2\hbar}\right) \ , \tag{3.18}$$

and $E = -W_0$. As pointed out in [24], (3.16) gives the eigenvalue equation for the tight binding model which describes electron motion in a quasirandom potential T_k with the hopping parameter W_k. The property of this model depends on the rationality of the coefficient of k in the potential. When the coefficient is irrational, the model is known to show Anderson localization.

We can now analyze the relation between the breaking of dynamical localization and quantum decoherence. Loss of quantum coherence is measured by the density matrix becoming approximately diagonal. Decoherence in the quantum Brownian model has been studied extensively for this problem [17]. In Fig. 3(a) we plot the linearized entropy $\mathrm{Tr}\rho_r^2$ versus the energy $\langle p^2/2\rangle$ in each diagram (we set the mass $m = 1$ for all the numerical calculations). Note that the two effects are correlated to each other as expected. This shows that delocalization occurs as the quantum coherence breaks down, suggesting that delocalization and decoherence occur by the same mechanism. As the noise strength increases, we see that decoherence works more efficiently. Also as the nonlinearity parameter K, the strength of the kick in this model, increases, the system decoheres more rapidly [Fig. 3(b)]. At the same time, the amount of delocalization measured by the diffusion constant also increases. For all the numerical results presented in this paper, we use the Gaussian wave packet as the initial condition. However, we also checked that the qualitative results given in this paper are insensitive to the initial condition. This may be viewed as another characteristic of a chaotic system. For QKR, as the nonlinear parameter K decreases, the results become more sensitive to the initial condition [29]. In nonchaotic systems, the sensitivity in this sense can be used to choose a preferred initial state in accordance with some specific criterion, such as least entropy production [30], etc. (For chaotic cases, see [31] for a related argument but from a different point of view.)

This may be explained in the following way. Because we use a coupling through the momentum, the time scale for the system to lose coherence is given by $t_{dec} = \frac{1}{\gamma}(\frac{\lambda_{tdB}}{\delta p})^2$, where $\lambda_{tdB} = h/\sqrt{2\pi mkT}$ is the thermal de Broglie wavelength, and δp is the relevant momentum scale. After this time, noise will destroy the quantum coherence between these momentum separations. In the kicked rotor case, localization will occur due to the coherence around $\delta p \sim \Delta$, where $\Delta \sim l\hbar$ is the localization length. Since $l \sim K^2$, this gives $t_{dec} \sim \frac{1}{K^4}$. Therefore nonlinearity increases the rate of decoherence.

The relation between the diffusion constant D and the noise strength is given in [26,28]. For our case, $K/\hbar \gg 1$ and for weak noises, we can consider the particle as undergoing a random walk with hopping parameter $1/t_c$. Then $D = \frac{\Delta^2}{t_{dec}}$, where Δ gives the localization length. From this, we get

$$D = \gamma\left(\frac{\Delta^4}{\lambda_{\theta dB}^2}\right) \ . \tag{3.19}$$

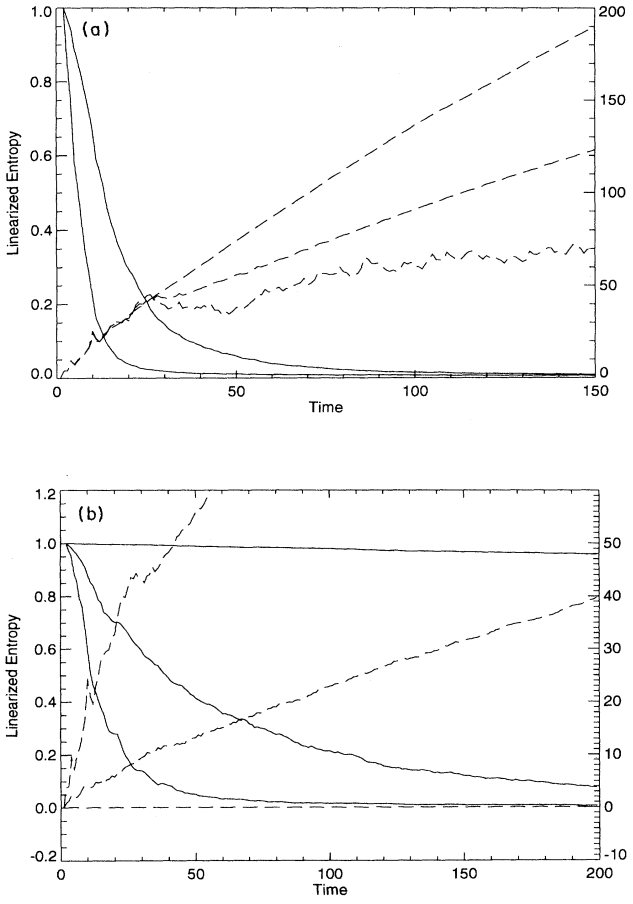

FIG. 3. $\mathrm{Tr}\rho_r^2$ (solid line, left scale) and $\langle p^2/2\rangle$ (dashed line, right scale) are plotted in (a) versus time for $K = 10$ and $\hbar = 1$. Three noise strength values $\sigma = 0$, $\sigma = 1.0$, $\sigma = 2.0$ are plotted here, corresponding to the family of lines from top to bottom for Tr ρ_r^2 and bottom to top for $\langle p^2/2\rangle$ (note that $\mathrm{Tr}\rho_r^2 = 1$ for $\sigma = 0$). As the noise strength increases, the decoherence time shortens, and $\mathrm{Tr}\rho_r^2$ decays rapidly. This accompanies the increase of diffusive behavior in $\langle p^2/2\rangle$. In (b), the same observables are plotted but with different K values. The upper, middle, and lower solid lines (lower, middle, and upper dashed lines) correspond to $K = 0.5$, $K = 5$, $K = 10$, respectively. Here $\sigma = 1.0$, $\hbar = 1$ are fixed. We see that increasing nonlinearity shortens the decoherence time. Note that when $K = 0.5$, the system merely diffuses.

IV. DECOHERENCE AND IRREVERSIBILITY

The Wigner function representation is often used to examine the quantum to classical transition. For a linear system the Wigner function is known to show a smooth convergence to the classical Liouville distribution. But if the system Hamiltonian has a nonlinear term, quantum corrections associated with the higher derivatives of the potential pick up the rapid oscillations in the Wigner function and it no longer has a smooth classical limit [40]. However, upon interaction with an environment, a coarse-grained Wigner function can have a smooth classical limit [41] for nonlinear systems.

The Wigner function at time $t = j$ is defined as

$$W_j(X,p) = \frac{1}{4\pi}\int_{-2\pi}^{+2\pi} dy\, e^{\frac{i}{\hbar}py}\,\rho_j\left(X-\frac{1}{2}y, X+\frac{1}{2}y\right), \tag{4.1}$$

where $X \equiv \frac{1}{2}(x+x')$, $y \equiv x - x'$. From (3.3), the unit-time propagator for the Wigner function of QKR is

$$W_{j+1}(X,p) = \exp\left[-\frac{K\sin X}{\hbar}\Delta_p\right] \times \exp\left[-\frac{p}{m}\partial_X\right] W_j(X,p)\ , \tag{4.2}$$

where $\Delta_p = \exp[\frac{\hbar}{2}\partial_p] - \exp[-\frac{\hbar}{2}\partial_p]$ measures the effect of the kick. We can see the effect of quantum corrections more clearly if we expand Δ_p in orders of $\hbar$:

$$\Delta_p = \exp\left[\frac{\hbar}{2}\partial_p\right] - \exp\left[-\frac{\hbar}{2}\partial_p\right] = \hbar\partial_p + \frac{\hbar^3}{24}\partial_p^3 + \frac{\hbar^5}{1920}\partial_p^5 + \cdots\ . \tag{4.3}$$

With this, the first exponential in (4.2) contains the classical propagator times quantum corrections of even orders of $\hbar$.

$$\exp\left[-\frac{K\sin X}{\hbar}\Delta_p\right] = \exp[-K\sin X\partial_p] \times \exp\left[-\frac{\hbar^2}{24}K\sin X\partial_p^3\right] \times \exp\left[-\frac{\hbar^4}{1920}K\sin X\partial_p^5\right]\cdots\ . \tag{4.4}$$

If the initial system wave function is described by a Gaussian wave packet with width $\delta p(\gg \hbar)$, we would expect to see a classical-like evolution of the packet at short times. When the width of the contracting wave packet gets small and becomes comparable to $\hbar$, the effect of quantum corrections, namely, the corrections from the exponents which are of higher order in $\hbar$ in (4.4) appears. By comparing the classical and the quantum terms, we can easily evaluate the length scale at which quantum corrections become important, i.e., when $\delta p(t) \sim \hbar$. Here $\delta p(t) = \delta p(0)e^{-\lambda t}$, where λ is the Lyapunov exponent given by $\lambda \sim \ln(K/2)$. As shown in (1.2), from this expression, we can define the time scale t_E as $t_E \sim \ln\frac{\delta p(0)}{\hbar}/\lambda$. Because the Wigner function or the expectation value of any observable follows classical trajectories when $t < t_E$, this has been called the Ehrenfest time. Note that in the continuum case, this definition gives us a different time scale for each term in the expansion [19]. Hereafter, we set $m = 1$ for brevity.

If the interaction with the environment takes the form (3.6), the major effect of the bath is the appearance of a diffusion term in (4.2), such that

$$W_{j+1}(X,p) = \exp[D_X\partial_X^2]\exp\left[-\frac{K\sin X}{\hbar}\Delta_p\right]\exp[-p\partial_X]W_j(X,p) \approx \exp[D_X\partial_X^2]\exp\left[-\frac{\hbar^3}{24}K\sin X\partial_p^3\right] W_j(X-p+K\sin X, p-K\sin X)\ , \tag{4.5}$$

where $D_X = 2M\gamma kT\hbar$ is related to a constant of the noise kernel $\nu(s)$ defined before (2.16).

Competition among the three terms with different physical origins is apparent: The first term in (4.5) is the quantum diffusion term, the second is the quantum correction term, and the third is purely classical evolution. As discussed by Zurek and Paz [19], if D_X is sufficiently large, the effect of quantum corrections becomes inconspicuous. In this case, the diffusion term traces out a small scale oscillating behavior before quantum corrections have a chance to change the classical evolution. Then one may expect the time evolution of the Wigner function to be like that of classical evolution with noise. In this case, we can ignore the quantum correction in (4.5) and write the evolution equation as

$$W_{j+1}(X,p) = \exp[D_X\partial_X^2] \times W_j(X-p+K\sin X, p-K\sin X). \tag{4.6}$$

The role of quantum diffusion is to add some Gaussian averaging so that the contracting direction in phase space will be suppressed while it does not affect the stretching direction. As long as the width of the wave packet is large such that the first term is negligible, the evolution should be Liouvillian (time reversible if we assume infinite measurement precision). Furthermore, we expect that after the width of the packet along the contracting direction becomes comparable to the diffusion generated width (in the Gaussian wave packet), the dynamics will start showing irreversible behavior arising from coarse graining (as distinct from irreversibility from instability). Consequently, entropy should increase in this regime. In Fig. 4, we plot the von Neumann entropy for the dynamics of (4.6). We can see three qualitatively different regimes: (I) the Liouville regime: the entropy is constant and the dynamics is time reversible; (II) the decohering regime: the entropy keeps increasing due to

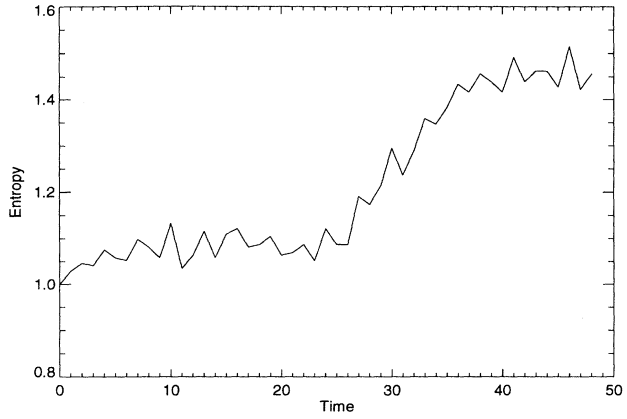

FIG. 4. The von Neumann entropy is plotted versus time for the kicked rotor. For the first 25 steps, the system does not produce any entropy. The evolution is reversible. Transition sets in the next few steps: the dynamics changes its character from reversible to irreversible. Because the nonlinear term is from the sinusoidal function, the onset of this regime is different at every phase space point. Consequently we can only see the averaged behavior through the entropy function. Around $t = 40$, saturation occurs due to the finiteness and the periodic nature of the phase space ($\sigma = 0.1$ for this case).

coarse graining; (III) the finite size regime: due to the bounded nature of the phase space, the entropy shows saturation. Our result from quantitative analysis seems to confirm the qualitative description of Zurek and Paz [19], who used the inverted harmonic oscillator potential as a generic source of instability. Since the phase space in their model is not bounded they do not see regime III. Similar features appear in the quantum cap map (Fig. 5). In this case, the full quantum dynamics can be calculated in a simple way. Resemblance with the result of a classical rotor with noise is obvious. However, in this case, the stable entropy is smaller than the maximum value which may be explained as a finite (phase space) size effect.

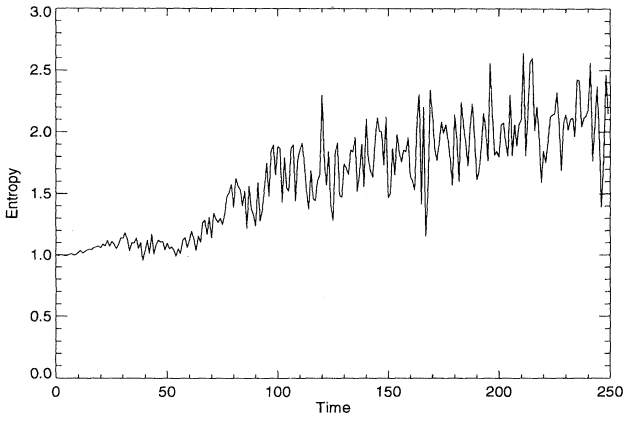

FIG. 5. The von Neumann entropy is plotted versus time for the quantum cat map. Due to the simplicity of the system, we see the same qualitative features as in Fig. 4. The entropy starts increasing around $t = 55$ and maintains a near-constant rate of production while showing large oscillations. After 200 steps, entropy production seems to saturate and starts decreasing into some stable value. $\mathcal{N} = 64$, $\sigma = 0.04$ are used here.

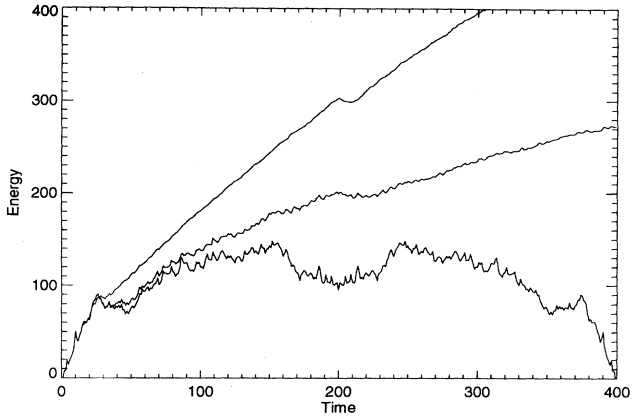

FIG. 6. The time reversal is performed at t=200. For QKR without a bath (lower curve), the system possesses time-reversal invariance [32]. When the interaction with the environment increases, the system gradually regains irreversibility as observed in classical systems. Here the noise strength $\sigma = 0.5$ (middle curve) and $\sigma = 1.0$ (upper curve). Also $\hbar = 1$, $K = 10$.

Quantum diffusion defined by the spreading of the wave function is known to be dynamically stable. The authors of [32] performed the time reversal at some time and saw the diffusion constant and even the wave function itself coming back to the same state within the accuracy of computation. As we know, these time-reversal behaviors cannot be seen in the classical case due to the instability of the trajectories. This is also true in real physical systems for which one can access information with only finite precision [2].

In Fig. 6, we perform the time reversal at $t = 200$. In the quantum case without bath, the system completely returns to the original state after exactly the same amount of time. Thus the system is highly stable in spite of its random appearance. On the other hand, in the classical case, instability prevents the reversibility even without interaction with the bath. When the interaction is turned on, we see that the reversibility in the quantum system is gradually lost, and irreversibility appears as the noise strength increases.

In a realistic physical system which has a finite precision due to numerical or instrumental limitation, we expect this type of irreversibility is inevitable for the chaotic system even without noise. If the minimum precision in length is denoted as ϵ, the time scale up to which the deterministic picture is valid is determined as $t_p \sim \frac{1}{\lambda} \ln \frac{2\pi}{\epsilon}$. At $t > t_p$, the system starts losing information about the past. This may be the source of irreversibility for the classical chaotic system. For the system we are studying, $t_p \gg t_E > 1$ holds. Then the quantum effect smears the contracting evolution of the region in the phase space before information about the past is lost. Therefore the wave packet traces back the same trajectory as it has traversed. If $t_c < t_p$, we see the irreversibility from coarse graining before the limitation

of the measurement becomes evident. This type of irreversibility is another characteristic of classicality peculiar to chaotic systems.

ACKNOWLEDGMENTS

We thank Dr. Shmuel Fishman and Dr. Juan Pablo Paz for explaining their work and Dr. Edward Ott and Dr. Richard Prange for general discussions. Research is supported in part by the National Science Foundation under Grant No. PHY91-19726. B.L.H. acknowledges support from the General Research Board of the Graduate School of the University of Maryland and the Dyson Visiting Professor Fund at the Institute for Advanced Study, Princeton. This work was completed while both authors enjoyed the hospitality of the physics department of HKUST.

[1] *Stochastic Behavior in Classical and Quantum Hamiltonian Systems*, edited by F. G. Casati, J. Ford, Lecture Notes in Physics Vol. 93 (Springer-Verlag, Berlin, 1979).
[2] J. Ford, Phys. Today **36**, 40 (1983).
[3] A. M. Ozorio de Almeida, *Hamiltonian Systems: Chaos and Quantization* (Cambridge University Press, New York, 1988).
[4] M. C. Gutzwiller, *Chaos in Classical and Quantum Mechanics* (Springer-Verlag, Berlin, 1990).
[5] *Chaos and Quantum Physics*, Les Houches Lectures Session LII, edited by M. J. Giannoni, A. Voros, and J. Zinn-Justin (North Holland, Amsterdam, 1991).
[6] A. J. Lichtenberg and M. A. Lieberman, *Regular and Chaotic Motion* (Springer-Verlag, Berlin, 1992).
[7] *Chaos and Quantum Chaos*, edited by W. Dieter Heiss, Lecture Notes in Physics Vol. 411 (Springer-Verlag, Berlin, 1992).
[8] *Quantum Dynamics of Chaotic Systems*, edited by J. M. Yuan, D. H. Feng, and G. M. Zaslavsky (Gordon and Breach, Langhorne, 1993).
[9] K. Nakamura, *Quantum Chaos* (Cambridge University Press, Cambridge, England, 1993).
[10] E. Ott, *Chaos in Dynamical Systems* (Cambrige University Press, Cambridge, England, 1993).
[11] Prog. Theor. Phys. Suppl. No. **116**, edited by K. Ikeda (1994).
[12] *Quantum Classical Correspondence*, edited by D. H. Feng and B. L. Hu (International Publishers, Boston, 1995).
[13] B. L. Hu and Yuhong Zhang, in *Quantum Dynamics of Chaotic Systems*, edited by J. M. Yuan, D. H. Feng, and G. M. Zaslavsky (Gordon and Breach, Langhorne, 1993).
[14] T. Kapitaniak, in *Chaos in Systems with Noise* (World Scientific, Singapore, 1990).
[15] R. E. Prange, in *Chaos and Quantum Chaos*, edited by W. Dieter Heiss, Lecture Notes in Physics Vol. 411, (Springer-Verlag, Berlin, 1992).
[16] J. A. Wheeler and W. H. Zurek, *Quantum Theory and Measurement*, edited by (Princeton University Press, Princeton, 1983).
[17] W. H. Zurek, Phys. Rev. D **24**, 1516 (1981); **26**, 1862 (1982); E. Joos and H. D. Zeh, Z. Phys. B **59**, 223 (1985); A. O. Caldeira and A. J. Leggett, Phys. Rev. A **31**, 1059 (1985); W. G. Unruh and W. H. Zurek, Phys. Rev. D **40**, 1071 (1989); B. L. Hu, J. P. Paz, and Y. Zhang, *ibid.* **45**, 2843 (1992); *ibid.* **47**, 1576 (1993); W. H. Zurek, Prog. Theor. Phys. **89**, 281 (1993).
[18] A. Tameshitit and J. E. Sipe, in *Quantum Dynamics of Chaotic Systems*, edited by J. M. Yuan, D. H. Feng, and G. M. Zaslavsky (Gordon and Breach Science Publishers, New York, 1992); Phys. Rev. A **45**, 8280 (1992); **47**, 1697 (1993).
[19] W. H. Zurek and J. P. Paz, Phys. Rev. Lett. **72**, 2508 (1994).
[20] T. Brun (unpublished).
[21] P. W. Anderson, Phys. Rev. **102**, 1008 (1958).
[22] M. R. Gallis and G. N. Fleming, Phys. Rev. A **42**, 38 (1990).
[23] F. G. Casati, B. V. Chirikov, F. M. Izrailev, and J. Ford, in *Stochastic Behavior in Classical and Quantum Hamiltonian Systems*, edited by F. G. Casati, J. Ford , Lecture Notes in Physics Vol. 93, (Springer-Verlag, Berlin, 1979).
[24] S. Fishman, D. R. Grempel, and R. E. Prange, Phys. Rev. Lett. **49**, 509 (1982); D. R. Grempel, R. E. Prange, and S. Fishman, Phys. Rev. A **29**, 1639 (1984); Phys. Rev. Lett. **49**, 833 (1982); S. Fishman, D. R. Grempel, and R. E. Prange, Phys. Rev. A **36**, 289 (1987).
[25] R. Graham, in *Chaos and Quantum Chaos*, edited by W. Dieter Heiss, Lecture Notes in Physics Vol. 411, (Springer-Verlag, Berlin, 1992), and references therein.
[26] D. Cohen and S. Fishman, Phys. Rev. A **39**, 6478 (1989); D. Cohen, *ibid.* **43**, 639 (1991); Phys. Rev. Lett. **67**, 1945 (1991).
[27] R. P. Feynman and F. L. Vernon, Ann. Phys. (N.Y.) **24**, 118 (1963).
[28] E. Ott, T. M. Antonsen, Jr., and J. D. Hanson, Phys. Rev. Lett. **53**, 2187 (1984).
[29] K. Shiokawa (unpublished).
[30] W. H. Zurek, S. Habib, and J. P. Paz, Phys. Rev. Lett. **70**, 1187 (1993).
[31] C. M. Caves, in *Quantum Classical Correspondence* eds. D. H. Feng and B. L. Hu (International Publishers, Boston, 1995).
[32] B. V. Chirikov, in *Chaos and Quantum Physics*, Les Houches Lectures Session LII, edited by M. J. Giannoni, A. Voros, and J. Zinn-Justin, (North-Holland, Amsterdam, 1991); D. L. Shepelyansky, *ibid.* **8**, 208 (1983); B. V. Chirikov, F. M. Izrailev, and D. L. Shepelyansky, *ibid.* **33**, 77 (1988).
[33] L. E. Ballentine, Y. Yang, and J. P. Zibin, Phys. Rev. A **50**, 2854 (1994).
[34] V. I. Arnold and A. Avez, *Ergodic Problems of Classical Mechanics* (Benjamin, New York, 1968).
[35] J. H. Hannay and M. V. Berry, Physica **1D**, 267 (1980).
[36] H. Kubotani, T. Okamura, and M. Sakagami, Physica A **214**, 560 (1995).
[37] A. O. Caldeira and A. J. Leggett, Physica **121A**, 587

(1983).
[38] H. Grabert, P. Schramn, and G. L. Ingold, Phys. Rep. **168**, 115 (1988).
[39] B. L. Hu, J. P. Paz, and Y. Zhang, Phys. Rev. D **45**, 2843 (1992); *ibid.* **47**, 1576 (1993).
[40] M. V. Berry, Philos. Trans. **287**, 237 (1977); E. Heller, J. Chem. Phys. **68**, 2066 (1978).
[41] K. Takahashi, Prog. Theor. Phys. Suppl. **98**, 109 (1989); S. Habib, Phys. Rev. D **42**, 2566 (1990).